TACK MEASUREMENTS OF PREPREG TAPE AT VARIABLE TEMPERATURE AND HUMIDITY

Christopher Wohl[1], Frank L. Palmieri[1], Alireza Forghani[2], Curtis Hickmott[2], Houman Bedayat[2], Brian Coxon[2], Anoush Poursartip[2,3], Brian Grimsley[1]

[1]NASA Langley Research Center, Hampton, VA, USA
[2]Convergent Manufacturing Technologies US, Seattle, WA, USA
[3]Department of Materials Engineering, The University of British Columbia, Vancouver, BC, Canada

ABSTRACT

NASA's Advanced Composites Project has established the goal of achieving a 30% reduction in the timeline for certification of primary composite structures for application on commercial aircraft. Prepreg tack is one of several critical parameters affecting composite manufacturing by automated fiber placement (AFP). Tack plays a central role in the prevention of wrinkles and puckers that can occur during AFP, thus knowledge of tack variation arising from a myriad of manufacturing and environmental conditions is imperative for the prediction of defects during AFP. A full design of experiments was performed to experimentally characterize tack on 0.25" slit-tape tow IM7/8552-1 prepreg using probe tack testing. Several process parameters (contact force, contact time, retraction speed, and probe diameter) as well as environmental parameters (temperature and humidity) were varied such that the entire parameter space could be efficiently evaluated. Mid-point experimental conditions (i.e., parameters not at either extrema) were included to enable prediction of curvature in relationships and repeat measurements were performed to characterize experimental error. Collectively, these experiments enable determination of primary dependencies as well as multi-parameter relationships. Slit-tape tow samples were mounted to the bottom plate of a rheometer parallel plate fixture using a jig to prevent modification of the active area to be interrogated with the top plate, a polished stainless steel probe, during tack testing. The probe surface was slowly brought into contact with the pre-preg surface until a pre-determined normal force was achieved (2-30 N). After a specified dwell time (0.02-10 s), during which the probe substrate interaction was maintained under displacement control, the probe was retracted from the surface (0.1-50 mm/s). Initial results indicated a clear dependence of tack strength on several parameters, with a particularly strong dependence on temperature and humidity. Although an increase in either of these parameters reduces tack strength, a maximum in tack was predicted to occur under conditions of low temperature and moderate humidity.

INTRODUCTION

Automated fiber placement (AFP) is a rapidly advancing method in the manufacture of composite parts.[1] As this technology has advanced, integration of composite parts into a variety of industries has increased in an effort to improve vehicle sustainability and environmental impact. However, for the aerospace community, certification of composite parts as either a replacement of existing structure or part of a new architecture is protracted. NASA is seeking to address this through the Advanced Composites Project (ACP) which has identified the goal of

reducing the timeline for certification of primary composite structure for commercial aircraft by 30%. This will be achieved through improvements in composite properties prediction, inspection, and manufacturing. Processes involved in the manufacture of composite parts using AFP are particularly sensitive to the properties of the prepreg itself. Fiber buckling, wrinkling, and a variety of other defects can have deleterious effects on the final composite part.[2-3] Computational modeling of the behavior of prepreg in a complex configuration can enable dramatic reduction in these manufacturing defects.[4] However, one property of particular significance, prepreg tack, has yet to be fully characterized, especially under an extended range of temperature and humidity conditions.

Characterization of prepreg tack has been achieved primarily through two techniques, probe[5-6] and peel.[7-8] In several of these studies, experimental and environmental parameters were varied to determine their influence on prepreg tack. However, these experiments were conducted by investigating a single parameter while the remaining parameters were kept constant. This necessarily eliminates the possibility of observing the influence of two parameters in conjunction on the property of interest. In this work, a design of experiments (DOE) approach to investigate the multivariate design space of several experimental and environmental parameters will be utilized to ascertain individual, crossed, and higher order term dependencies on several experimental results collected using probe tack testing.

EXPERIMENTATION

1.1 Materials and Methods

The prepreg used for tack characterization was 0.25" slit-tape tow IM7/8552-1. Prior to testing, the prepreg material was held in a freezer at -8 °C unless removed for sample cutting and preparation, which was conducted under ambient conditions (~ 20 °C). The samples were exposed to ambient conditions prior to testing for approximately 24 h as a result of removal of the material from the freezer and generation of sample specimens. This was held nearly constant for all samples to minimize the uncertainty in results that would be related to advancing of the epoxy resin.

Samples were prepared for tack testing by adhering the prepreg onto a sand-blasted rheometer lower flat plate (stainless steel, 50 mm diameter) using a custom-built fixture (Figure 1A). This fixture was designed to enable uniform pressure to be applied over the interaction area between the prepreg tape and the sand-blasted plate. The fixture consisted of a stainless steel flat plate with a circular cavity in the middle to accommodate the region that would be interrogated by the probe during the tack test. Alignment pins were integrated into the flat plate to maintain the approximate location of the interrogation region. Rubber washers (three, 50 mm diameter) were included in the sample preparation configuration to further equalize pressure distribution (Figure 1B). To prepare a sample for tack testing, the rubber washers were placed within the alignment pins of the stainless steel flat plate. Next, the prepreg tape (approximately 55 mm in length) was carefully placed across the central portion of the rubber washers. Two different probe diameters were used for tack testing (4 and 8 mm) which required a single piece of prepreg tape for the 4 mm probe test configuration and two pieces of prepreg tape for the 8 mm probe test configuration. Great care was taken to ensure that the two pieces of prepreg tape were as closely oriented as possible with no overlap or gap that would interfere with the tack testing.

The sand-blasted plate was placed on top of the affixed prepreg tape. This assembly was placed into a bench-top press (Carver laboratory press, model C) and compressed to 66 psi. The uniformity of the pressure distribution was confirmed using pressure sensitive film (Figure 1C, Sensor Products, Inc).

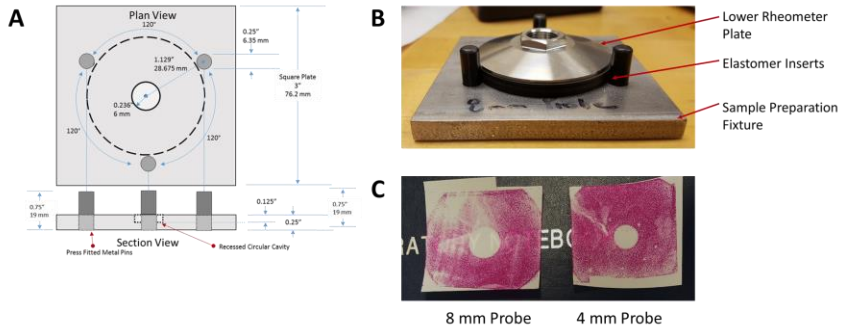

Figure 1. (A) Schematic of sample preparation fixture. (B) Assembled components for sample preparation. (C) Image of pressure sensitive film utilized for pressure distribution visualization with the 8 mm (left) and 4 mm (right) probe sample preparation fixtures.

Probe tack testing was performed using an Anton Paar USA Inc. MCR 520 TwinDrive™ Modular Rheometer equipped with an environmental controller (MHG 100 Humidty Generator). Two probe diameters were utilized for this work (4 and 8 mm) that were supplied by the vendor and calibrated for actual diameter and mass. Through the course of a single experiment, several steps were completed including: equilibration to the desired test temperature and humidity conditions, approach of the probe ending in contact with the prepreg at a preset normal force, a probe-prepreg contact hold time, and finally, retraction of the probe from the surface during which the tack strength was measured (Figure 2). In an effort to minimize experimental error, the probe was brought close to the surface, within 5 mm, prior to changing the environmental conditions. Likewise, the desired temperature was achieved prior to changing relative humidity conditions. A step-wise approach to increasing humidity was also performed to reduce temperature variation through the course of attaining the desired environmental condition. Finally, there are two methodologies to control the probe configuration while in contact with the sample, i.e., during the contact hold time. Using displacement control, the normal force will decrease during the contact hold time as the epoxy resin flows away from the contact area. For these experiments, the normal force (F_N) after the hold period (contact time) was recorded for analytical purposes. Using load (normal force) control, the displacement of the probe is adjusted to maintain a constant normal force; thus, as resin flows away from the contact area, the probe is lowered to retain the desired normal force. Both methods were utilized in this work. As such, there are several experimental parameters that can be changed to interrogate their influence on tack strength.

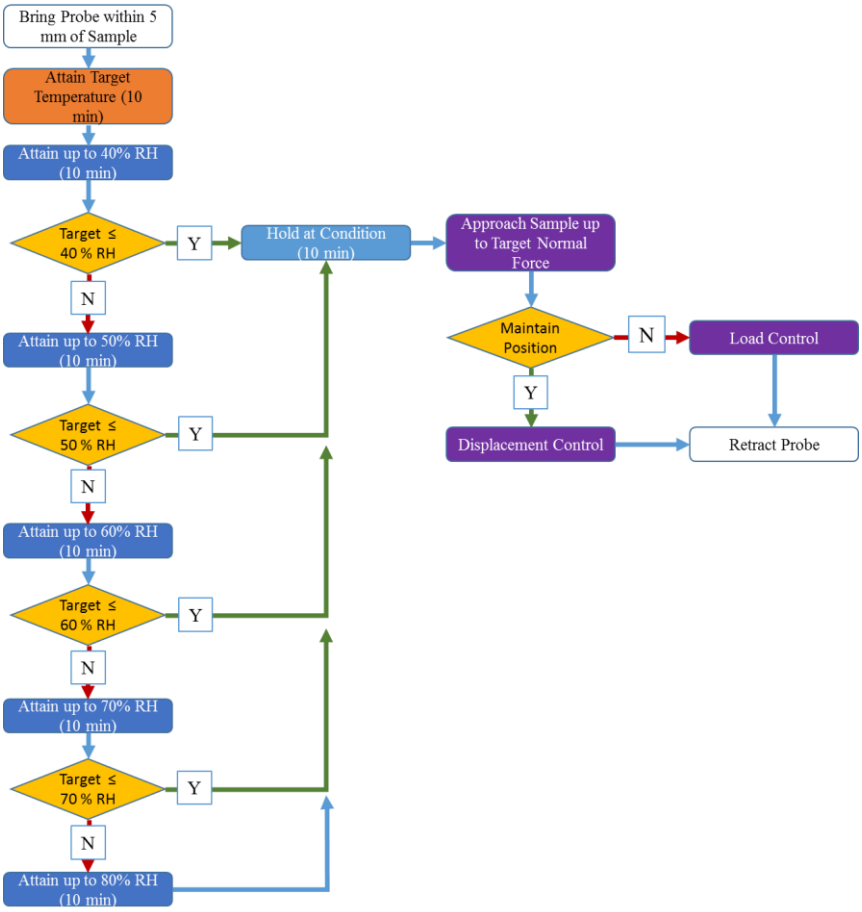

Figure 2. Sequence of steps involved in a single probe tack test experiment.

1.2 Evaluation of Parameter Space via Design of Experiments

As can be seen in Figure 2, there are several experimental parameters that can be changed to interrogate their influence on tack strength. To exhaustively explore every potential combination of parameters is impractical. Evaluation of 5 variables with 5 discrete levels (contact hold time, contact force, crosshead speed, temperature, and relative humidity) and 1 variable with 2 levels (probe diameter) would result in 6250 different experimental conditions. Therefore, a DOE approach was utilized. Using a response surface model with inclusion of extrema and intermediate values as well as built-in repeated runs to test reliability, a total of 95 experimental conditions were identified as necessary to build a model that would enable statistically significant navigation of this design space. As can be seen in Table 1, all of the variables were categorized as numerical and continuous, except for probe diameter which was set as categorical, to enable the greatest flexibility in identification of experimental parameters. A full list of the experimental parameters investigated in this work can be seen in Appendix A.

Table 1. List of input factors utilized for DOE project generation.

Factor	Parameter	Units	Type	Subtype	Minimum	Maximum

A	Contact Time	s	Numeric	Continuous	0.01	10
B	Scaled Contact Force	N/mm^2	Numeric	Continuous	2	30
C	Crosshead Speed	mm/s	Numeric	Continuous	0.1	50
D	Temperature	°C	Numeric	Continuous	25	80*
E	Relative Humidity (%RH)	%	Numeric	Continuous	20	80*
F	Probe Diameter	mm	Categoric	Nominal	4	8

*Due to limitations of the environmental chambers, the following restrictions were enforced on the DOE:
(1) %RH could not exceed 50% at 80 °C
(2) %RH could not exceed 70% at 70 °C

Responses extracted from the data streams were identified based on the utility of each factor to provide further insight into the processes involved in retraction of the probe from the surface. Beyond the obvious identification of the actual temperature and humidity that was achieved during the test, the maximum adhesion force (F_{Adh}) and the integrated area of the force-displacement curve (A) were also of interest. To make all of the collected data sets comparable, these values were scaled according to the probe area. Similarly, the nature of the sample response, e.g., a sharp inelastic response with minimal fibrillation vs an elastic response with a portion of the adhesion force retained over greater gap distances, was of interest. Initially, line shape analysis was performed; however, the line shape variability was too great to enable uniform curve fitting across different experimental conditions. Therefore, relative gap distances were determined according to the following:

$$\Delta d_{50} = d_{50} - d_{100} \quad (1)$$

$$\Delta d_{25} = d_{25} - d_{100} \quad (2)$$

where d_{100}, d_{50}, and d_{25} are the gap distances at 100%, 50%, and 25% of F_{Adh} measured as the probe is retracted from the surface after contact. For surfaces with rapid decohesion, the Δd_{50} and Δd_{25} values should be very small: surfaces with fibrillation and more gradual decohesion should yield larger Δd_{50} and Δd_{25} values.

Table 2. List of responses utilized for statistical analysis.

Response	**Units**
% Normal Force after Hold ($F_{\%N}$)	n/a
Scaled Adhesion Force (F_{Adh})	N/mm^2
Scaled Integrated Area (A)	N/mm
Gap Distance at 100% F_{Adh} (d_{100})	mm
Gap Distance at 50% F_{Adh} (Δd_{50})	mm
Gap Distance at 25% F_{Adh} (Δd_{25})	mm

Collectively, these inputs and responses were integrated into the DOE software (Design Expert 9.0, Stat-Ease Inc.) to generate a series of prediction models for the various response parameters. Depending on the model utilized, linear and quadratic dependencies on the input parameters can be elucidated; higher order dependencies can also be revealed but typically don't

demonstrate a strong correlation with the data. Likewise, cross-term dependencies, that is, dependencies that are the product of two inputs, can be identified. Once completed, a response surface can be generated to ascertain the relative contributions from two inputs on a single output in a continuous fashion. It should be noted that this was of particular interest for this work as the interdependency between temperature and humidity on adhesion strength had not been systematically studied to the best of the authors' knowledge at the time this was written.

RESULTS AND DISCUSSION

Through the use of DOE, a total of 95 different combinations of test conditions were utilized to measure the tack and response properties of uncured IM7/8552-1 prepreg samples. The specific parameters for each test condition from the DOE are provided in Appendix A. The values for the response parameters are provided in Appendix B. As a result of these experiments, the influence that each input parameter has, as well as combinations of input parameters, on the tack and response of the prepreg sample can be evaluated. The following section will discuss the results from analysis of this data in increasing complexity.

1.3 Probe Tack Test Experimental Results: Empirical Trends

As described previously, the shape of the force-displacement curve can provide information regarding the nature of the prepreg-probe interaction as the probe is retracted from the surface. Shown in Figure 3 is an example of data collected through the course of the experiments identified through the use of DOE. The conditions that this data were collected at (relatively high temperature and humidity with moderate values for the remaining parameters) will be described later in this text to be likely to result in a strong adhesion interaction. As can be seen, the increase in adhesion force is rapid during initial retraction, reaches a peak, and then partially diminishes in a similarly rapid manner. This can be related to the formation of fibrils (cavitation) as the resin itself retains continuous filaments between the probe and prepreg surfaces. As the retraction continues, these filaments elongate and ultimately break returning the adhesion force to the baseline. Differences in test conditions will dramatically influence both the magnitude and shape of this curve.

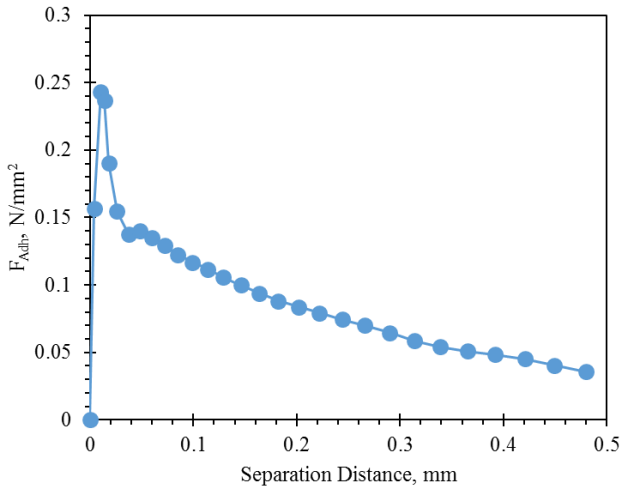

Figure 3. An example force-displacement curve from probe tack testing. The conditions utilized for this experiment are indicated in Appendix A (Run 8).

1.4 Statistical Analysis of Probe Tack Test Experimental Results

One of the most critical aspects of utilizing a DOE approach to explore variable space is the robustness of the data collected and the models developed from that data. To that end, input parameter values were chosen for experimental runs to include both extrema as well as intermediate points, i.e., input parameter values that fall somewhere between the maximum and minimum values. This enables development of models describing the response of the system that include curvature.

Analysis of experimental results (responses) is also a critical consideration when determining the robustness of the collected data and capability of utilizing this data to generate meaningful models to describe the variable space that was explored. Thus, repeatability of the data is important as it will indicate the confidence in the values obtained for the entirety of the DOE. For the particular experiments conducted in this work, this was of greater significance as a result of the categorical input parameter, probe diameter. As both 4 mm and 8 mm diameter probes were used, the repeatability of measurements using each probe was an important consideration and the resultant F_{Adh} values are shown below (Table 3). Another useful insight this data can provide is whether or not there is a statistically significant difference between the data collected with the 4 mm probe compared to the 8 mm probe. To ascertain this, a t-test was performed on the F_{Adh} average values obtained for each probe. In this analysis, a null hypothesis is considered that there is no statistically significant difference between the two mean values taking into consideration the number of data points (degrees of freedom), the mean value, and an estimated standard error (calculated using the standard deviation values attributed to each mean). The resultant p-value (likelihood that the null hypothesis is correct) was 0.57. This indicated that there is a 57% chance that the difference between these two mean values is not statistically significant. P-values less than 0.05 are often considered necessary to consider the difference between two mean values to be significant, thus we can consider the average F_{Adh} values obtained for each probe to not be statistically significant. This is a very important result as it further validated the opportunity to collect meaningful data through this DOE since, at least from a macroscopic perspective, if the F_{Adh} data is scaled according to contact area of the probe, the results should be independent of contact area. Furthermore, this result enabled the distinction between probe diameter utilized to collect the data to be removed improving the depth and continuity of the data collected in this DOE.

Table 3. F_{Adh} values measured for center-point repeat runs conducted with the 4 mm and 8 mm probes.

Trial Number	F_{Adh}, 4 mm Probe* (N/mm^2)	F_{Adh}, 8 mm Probe* (N/mm^2)
1	0.35 (9)	0.29 (8)
2	0.44 (46)	0.27 (12)
3	0.49 (48)	0.33 (41)

4	0.23 (54)	0.30 (64)
5	0.40 (63)	0.32 (82)
6	0.45 (72)	--
Average	0.39 ± 0.09	0.30 ± 0.02

*The actual experimental run number that the repeat run was conducted at is indicated in parenthesis.

With this level of confidence established in the collected data, the data collected for each response parameter was fitted to a model according to which model was determined to be the most statistically relevant. Linear, quadratic, cubic, as well as custom models were all considered and potentially applicable due to the input parameter variation built into the DOE. Ultimately a quadratic model was considered for each response in order to minimize model complexity and maximize accuracy. Often transforms, mathematical operations performed on the response value, are utilized to further explore the nature of the model being developed. Which transform was incorporated was determined based on statistical analysis of each possible permutation. Once the model and transform were established, the significance of each input parameter as well as more complex parameters based on the quadratic model (i.e., cross input parameters and the square of each input parameter) was determined. The results of this analysis are presented in Table 4. The relative significance of each input parameter is indicated by the color of the cell. This was determined by considering the scaled model generated in the Design Expert software, where the level of significance varied from -1 to 1. The closer the input parameter coefficient (C_{IP}) was to zero, the lower the significance of that term. Coefficients with values < 0.05 were considered to be entirely insignificant and were not included; if the coefficient was considered to not be significant for any of the response models, it was excluded from the table entirely (i.e., AB, AC, etc.). The color for each cell is indicative of the magnitude of the coefficient according to the following: red ($0.06 \leq C_{IP} \leq 0.15$), orange ($0.16 \leq C_{IP} \leq 0.30$), yellow ($0.31 \leq C_{IP} \leq 1.00$), green ($C_{IP} > 1$). Although the significance of some of the included input parameters is low (red blocks), many of them were included to retain hierarchical design if higher order terms (cross terms or the square of a single term) were determined to be significant. The sign of the coefficient is also indicated in Table 4 and indicates whether there was a direct or inverse relationship between that input parameter and the response value.

Table 4. Magnitude of input parameter coefficients determined from scaled models. The color scale was: red ($0.06 \leq C_{IP} \leq 0.15$), orange ($0.16 \leq C_{IP} \leq 0.30$), yellow ($0.31 \leq C_{IP} \leq 1.00$), green ($C_{IP} > 1$)

Response	**F_{Adh}**	**F_N**	**A**	**d_{50}**	**d_{25}**
Model Transform	Square Root	None	Log	Log	Square Root
A	+*	-	+	-	+
B	-	-	-	+	-
C	+		+		
D	-	-	-	+	+
E	+	-	-	+	-
AD	-		-		

BC	+				
BD	-	-	-		
BE	+		-		
CD	+				
DE	-	-	-	-	-
A^2	-	+	-	-	-
B^2	-	-	-	+	
D^2	-		-	-	-
E^2	-		-		

*The sign of the coefficient indicates whether there was a positive or negative relationship between that input parameter and the response value.

One final consideration prior to analyzing what information can be obtained from this DOE and statistical analysis is evaluation of the agreement between predicted response values and actual response values. As can be seen in Figure 4, there was significant agreement between the two sets of values correlated to F_{Adh}. Similar responses were observed for the other response parameters. Through this final analytical step, the relevance and reliability of the models developed was determined to be significant indicating that the models can be utilized to ascertain relationships between the input and response parameters.

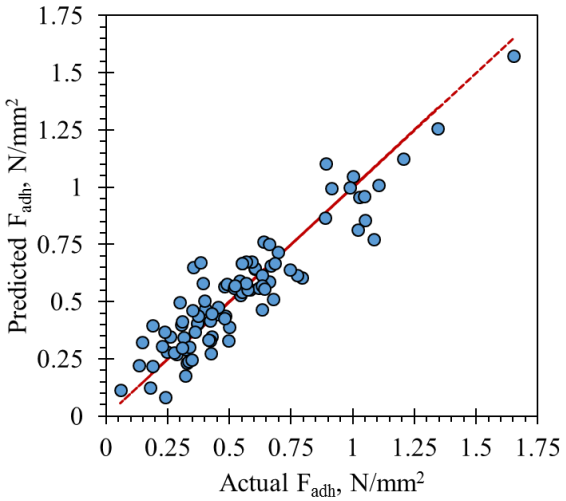

Figure 4. Comparison of F_{Adh} obtained experimentally and from the developed DOE model.

Shown in Figure 5, the relationships relative humidity had with several responses were determined. To generate these plots, the remaining experimental conditions were held constant at the following values: T = 40 °C, contact time = 10 s, contact force = 1 N/mm^2, crosshead speed = 25 mm/s. As can be seen, both the adhesion force and the integration area were found to have maxima at intermediate relative humidity values.

This can be understood as an increase in viscoelasticity of the resin. As the relative humidity increased from low to moderate values (up to approximately 50-60%) both F_{Adh} and A increased, which can be understood as an increase in the "tack" of the pre-preg. However, as the relative humidity continued to increase, the response time of the resin diminished (i.e., the viscosity of the resin decreased). As a result, the resin readily elongated and detached from the retracting probe surface resulting in reduced F_{Adh} and A values. This is further illustrated by the plots in Figure 5B and 5D which depict inverse trends for relative humidity change when comparing $F_{\%N}$ to d_{25}. Increased relative humidity resulted in a linear decrease in the $F_{\%N}$ value which suggested that the resin flowed out of the contact area to a greater degree under high relative humidity conditions. However, the d_{25} value increased with increased relative humidity value indicating that the resin remained in contact with the probe surface at greater separation distances. Collectively then, it should not be surprising that the F_{Adh} and A values exhibited maxima at intermediate relative humidity conditions.

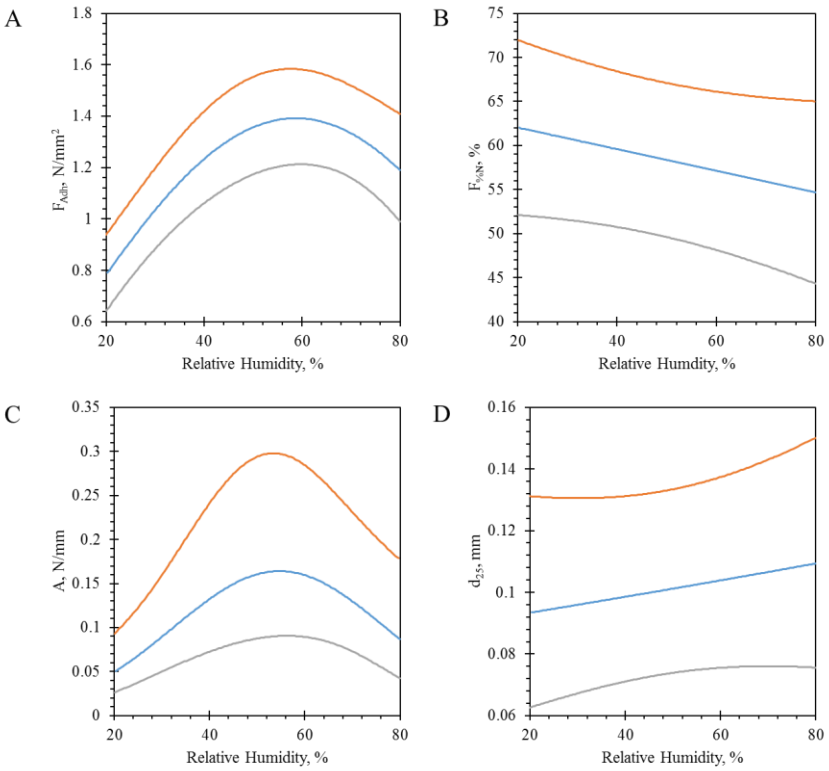

Figure 5. Response curves for variation in (A) F_{Adh}, (B) $F_{\%N}$, (C), A, and (D) d_{25} with respect to change in relative humidity. The model line in each plot is the blue line and the upper band (orange) and lower band (gray) are the upper and lower 95% confidence intervals.

Of even greater interest is how two input parameters (experimental conditions) affected a response parameter. The combined impact that changes in relative humidity and other input parameters had on F_{Adh} is displayed in Figure 6. Similar to the previous

plots, unless the input parameter is one of the axes in the plot the following conditions were utilized: T = 40 °C, contact time = 10 s, contact force = 1 N/mm^2, crosshead speed = 25 mm/s. Increased contact time resulted in an increase in F_{Adh}, with increasing relative humidity progressing through a maximum at intermediate values (Figure 6A). Interestingly, an increase in contact force progressed through a maximum at intermediate values (Figure 6B) indicating that the resin began to flow out of the contact area once a threshold contact force was reached. This threshold value was relative humidity dependent and varies from approximately 1.3 N/mm^2 at 20% RH to 1.7 N/mm^2 at 80% RH. Resin viscosity influence on F_{Adh} was even more pronounced when considering changes in both temperature and relative humidity (Figure 6C). There was a clear decrease in F_{Adh} as the temperature increased and this effect even superseded the increase in F_{Adh} values at high relative humidity settings. It should be noted that changes in F_{Adh} with crosshead speed (probe retraction rate) did not exhibit a maximum at intermediate values (data not shown) which was observed by Crossley et al. (it should be noted these results were from a peel experiment).[7] The range of velocities used in this work exceeded those evaluated by Crossley and therefore would not have enabled observation of this behavior. Thus, according to the conditions utilized in this DOE, a maximum F_{Adh} value would be anticipated when the contact time was greatest, the contact force and relative humidity were moderate, and the temperature was relatively low with little influence from crosshead speed. In the next section, the statistical optimization conditions will be discussed.

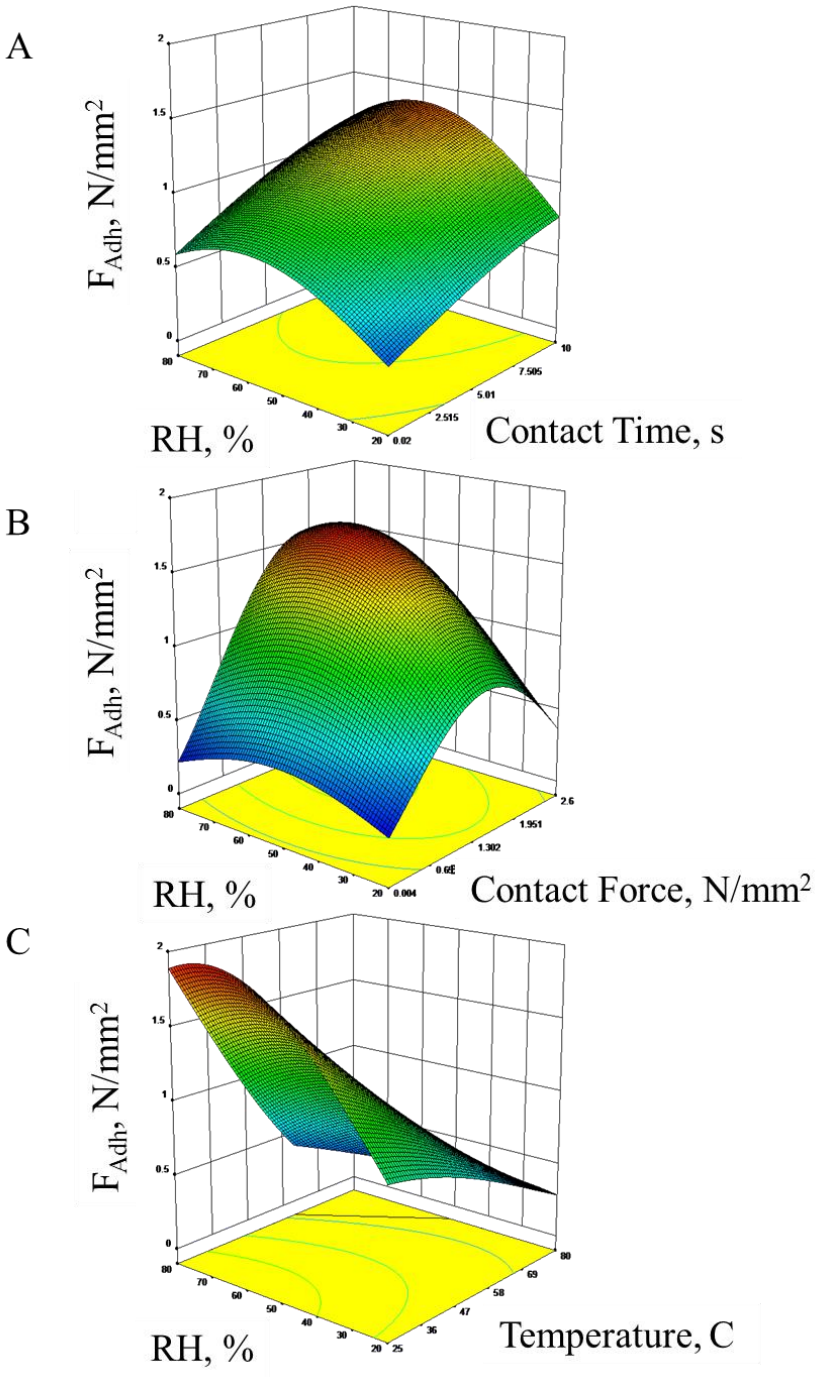

Figure 6. Response surfaces for variation in F_{Adh} with respect to change in relative humidity and (A) contact time, (B), contact force, and (C) temperature.

Optimization analysis was utilized in an effort to identify (statistically) the experimental conditions that maximized F_{Adh}. This analysis is performed by first setting what the target response conditions should be. In this analysis, maximum values for both F_{Adh} and A were utilized. From the input parameters and correlated response results, the most desirable conditions are identified and plotted as a function of desirability, which

can be utilized to further explore the design space. As can be seen in Figure 7A, the desirability was greatest for relatively low temperature values and moderate to high relative humidity conditions. Furthermore, the Design Expert software will calculate a series of input parameter conditions that will provide diminishing values of desirability. The temperature and relative humidity exhibited nominal change through 50 different optimized input conditions (Figures 7B and 7C) indicating that the desirability was strongly influenced by these parameters. Conversely, the crosshead speed was initially near the upper limit but became increasingly varied indicating that this parameter did not significantly influence the developed model.

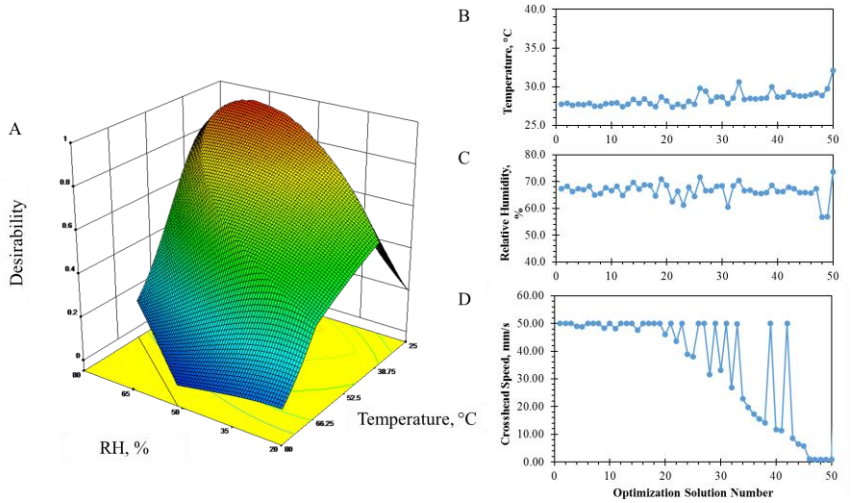

Figure 7. (A) Optimization plot for maximizing F_{Adh}. The change in input parameters (B, temperature; C, relative humidity; D, crosshead speed) provided additional insight into their influence on the desirability value.

CONCLUSIONS

Design of experiments provided a critical, statistically relevant, pathway to efficiently explore the design space incumbent for investigating prepreg tack. A series of input parameters (experimental conditions) were utilized to generate test conditions and a series of response parameters were recorded at each condition. Ultimately, the influence that relative humidity and temperature have on prepreg tack, as environmental conditions, as well as several experimental configuration conditions were determined. Although an increase in relatively humidity improved tack strength, F_{Adh}, an increase in temperature or exceeding a threshold contact force value reduced or, in some cases, completely negated that change. Contact time was determined to be beneficial for increasing tack strength, while crosshead speed (probe retraction rate) was determined to play a minimal role for the range of velocities investigated here. These results may provide useful insight into the nature of prepreg systems under a variety of environmental

and experimental conditions as the methods of composite parts manufacture continue to improve and evolve and the use of composite materials continues to proliferate. Although these experiments measured tack forces between a prepreg surface and a stainless steel probe, future work will investigate interactions between two prepreg surfaces via a peel test configuration.

REFERENCES

1. Lukaszewicz, J. A.; Ward, C.; Potter, K. D., The Engineering Aspects of Automated Prepreg Layup: History, present and future. *Composites: Part B* **2012,** *43*, pp 997-1009.

2. Beakou, A.; Cano, M.; Le Cam, J. B.; Verney, V., Modelling Slit Tape Buckling During Automated Prepreg Manufacturing: A Local Approach. *Composite Structures* **2011,** *93*, pp 2628-2635.

3. Kim, B. C.; Weaver, P. M.; Potter, K. D., Manufacturing Characteristics of the Continuous Tow Shearing Method for Manufacturing of Variable Angle Tow Composites. *Composites : Part A* **2014,** *61*, pp 141-151.

4. Forghani, A.; Hickmott, C.; Houman, B.; Wohl, C.; Grimsley, B.; Coxon, B.; Poursartip, A. In *A Physics-Based Modelling Framework for Simulation of Prepreg Tack in AFP Process*, SAMPE Technical Conference, Seattle, WA United States of America, May 22-25, 2017.

5. Dubois, O.; Le Cam, J. B.; Beakou, A., Experimental Analysis of Prepreg Tack. *Experimental Mechanics* **2010,** *50*, pp 599-606.

6. Gillanders, A. M.; Kerr, S.; Martin, T. J., Determination of Prepreg Tack. *Internation Journal of Adhesion and Adhesives* **1981,** *1* (3), pp 125-134.

7. Crossley, R. J.; Schubel, P. J.; De Focatiis, D. S. A., Time-Temperature Equivalence in the Tack and Dynamic Stiffness of Polymer Prepreg and its Application to Autmoated Composites Manufacturing. *Composites: Part A* **2013,** *52*, pp 126-133.

8. Endruweit, A.; De Focatiis, D. S. A.; Ghose, S.; Johnson, B. A.; Younkin, D. R.; Warrior, N. A. In *Characterization of Prepreg Tack to Aid Automated Material Placement*, SAMPE Technical Meeting, Long Beach, CA United States of America, May 23-26, 2016.

APPENDIX A

DOE input parameters.

Run #	Contact Time, s	Scaled Contact Force, N/mm^2	Crosshead Speed, mm/s	Temperature, °C	Relative Humidity, %	Probe Diameter, mm
1	10	2	28.27	55.25	20	4
2	5.01	30	50	80	20	4
3	10	17.14	27.73	25	20	4
4	10	30	25.03	80	50	8
5	4.56	2	5	60	80	8
6	0.02	15.06	50	25	80	4

7	0.02	2	21.71	25	59.1	4
8	5.01	16	27.5	54	50	8
9	5.01	16	27.5	54	50	4
10	10	2	50	80	50	4
11	6.01	2	50	80	20	8
12	5.01	16	27.5	54	50	8
13	10	30	5	56.9	20	8
14	10	30	50	60	80	8
15	10	2	5	50.50	20	8
16	7.01	19.5	5	80	50	4
17	10	2	5	25	80	4
18	10	30	30.88	80	20	4
19	10	2	28.85	25	80	8
20	10	30	5	25	80	8
21	0.02	30	5	25	80	4
22	10	18.1	50	80	20	8
23	0.02	30	23	25	20	8
24	4.56	16.42	5	25	20	8
25	0.02	2	50	43.15	43.4	8
26	10	2	28.27	55.25	20	4
27	5.01	30	50	80	20	4
28	10	2	50	25	20	8
29	0.52	3.4	5	73.95	58.4	4
30	10	30	5	60	80	4
31	3.36	2	24.35	80	20	8
32	0.77	16.80	46.63	25	25.1	8
33	7.43	13.2	50	61.03	27.1	4
34	7.02	30	19.70	30.5	32.5	8
35	0.02	30	50	25	20	4
36	10	2	5	80	50	8
37	4.08	2	50	25	20	4
38	5.23	2	5	60	80	4
39	4.61	30	5	80	20	8
40	10	9.35	5	80	20	4
41	5.01	16	27.5	54	50	8
42	10	12.98	50	60	80	4
43	0.02	30	28.95	80	50	4
44	2.05	30	50	60	80	4
45	10	30	50	25	80	4
46	5.01	16	27.5	54	50	4
47	10	30	5	25	20	4
48	5.01	16	27.5	54	50	4
49	10	30	5	60	80	4
50	10	30	50	25	20	8
51	0.02	30	5	48.83	29	4
52	6.56	3.54	5.23	54.50	39.5	4
53	0.02	30	5	60	80	8
54	5.01	16	27.5	54	50	4
55	3.36	2	24.35	80	20	8
56	0.02	2	5	39.85	47	8
57	5.61	19.64	50	44.25	46.7	8
58	4.76	30	29.75	25	80	8
59	0.02	30	50	25	60.2	8
60	0.02	13.62	5	80	50	8
61	0.02	2	50	80	50	4
62	10	2	50	25	57.5	4
63	5.01	16	27.5	54	50	4
64	5.01	16	27.5	54	50	8
65	0.07	23.43	28.31	25	49.3	4

66	3.63	2	5	25	20	4
67	0.22	21.54	22.55	53.30	78.8	4
68	10	12.92	32	60	80	8
69	0.02	2	26.02	59.925	80	4
70	0.02	2	26.6	25	20	8
71	0.02	30	50	80	50	8
72	5.01	16	27.5	54	50	4
73	5.01	2	50	25	80	8
74	10	30	50	46.42	40.7	4
75	0.02	12.81	50	52.5	20	4
76	0.02	2	50	60	80	8
77	0.02	13.76	5	25	80	8
78	10	14.32	5	25	49.1	8
79	10	29.02	38.75	31.6	58.5	8
80	0.02	30	26.6	56.63	20	8
81	4.80	30	5	25	50	4
82	5.01	16	27.5	54	50	8
83	9.501	2	40.78	54.43	46.0	8
84	6.82	14.95	30.65	25	80	4
85	0.02	19.25	5	80	20	4
86	0.02	2	5	80	20	4
87	0.02	15.44	50	80	20	8
88	10	3	1	80	20	8
89	10	3	1	54	50	4
90	0.02	30	1	80	20	8
91	0.02	30	1	54	50	4
92	10	3	0.1	80	20	8
93	10	3	0.1	54	50	4
94	0.01	30	0.1	54	20	8
95	0.02	30	0.1	54	50	4

APPENDIX B

DOE response parameters.

Run #	**$F_{\%N}$**	**F_{Adh}, N/mm^2**	**A, N/mm**	**d_{100}, mm**	**d_{50}, mm**	**d_{25}, mm**
1	0.2600	0.2029	0.01409	0.164	0.18	0.226
2	0.4573	0.3645	0.02579	0.133	0.146	0.192
3	0.6038	1.1037	0.01225	0.177	0.177	0.177
4	0.6340	0.2509	0.01761	0.122	0.127	0.179
5	0.4400	0.0181	0.00092	0.155	0.171	0.197

6	0.9697	0.9772	0.00659	0.163	0.163	0.163
7	0.6750	0.1377	0.00037	0.163	0.163	0.163
8	0.7188	0.2932	0.05407	0.15	0.225	0.532
9	0.2963	0.3501	0.07033	0.183	0.399	0.515
10	0.2050	0.1066	0.00466	0.115	0.144	0.161
11	0.2650	0.0567	0.00500	0.119	0.165	0.231
12	0.5475	0.2690	0.09579	0.119	0.35	0.649
13	0.6517	0.6024	0.11596	0.109	0.166	0.423
14	0.4480	0.2310	0.01817	0.085	0.108	0.201
15	0.2150	0.1615	0.02075	0.136	0.236	0.325
16	0.1615	0.2467	0.01229	0.098	0.102	0.15
17	0.2450	1.1770	0.07040	0.151	0.162	0.195
18	0.4917	0.3398	0.00693	0.089	0.089	0.11
19	0.1550	0.1247	0.00777	0.159	0.174	0.247
20	0.7910	0.7918	0.00820	0.149	0.149	0.149
21	1.1253	1.2223	0.00667	0.149	0.149	0.149
22	0.4978	0.1379	0.00698	0.157	0.187	0.221
23	1.1780	0.0360	0.00041	0.145	0.145	0.145
24	0.5658	0.0957	0.00015	0.14	0.14	0.14
25	0.7800	0.0826	0.00248	0.147	0.155	0.189
26	0.4800	0.4011	0.06604	0.168	0.28	0.455
27	0.4340	0.3645	0.01419	0.113	0.118	0.149
28	0.1150	0.0217	0.00014	0.141	0.141	0.147
29	0.5853	0.1122	0.00504	0.144	0.176	0.206
30	0.2943	0.3239	0.03022	0.13	0.14	0.315
31	0.6500	0.0674	0.00351	0.141	0.182	0.192
32	0.8861	0.1196	0.00072	0.146	0.146	0.152
33	0.1727	0.2952	0.05994	0.138	0.318	0.5
34	0.7880	1.0437	0.01277	0.18	0.18	0.18
35	1.1180	0.0939	0.00347	0.2	0.2	0.2
36	0.3050	0.0360	0.00103	0.139	0.167	0.175
37	0.1100	0.0326	0.00008	0.153	0.153	0.155
38	0.2050	0.1035	0.00833	0.143	0.218	0.245
39	0.8497	0.2059	0.00723	0.152	0.171	0.204
40	0.1891	0.1830	0.01305	0.128	0.183	0.206
41	0.5231	0.3277	0.07016	0.156	0.208	0.489
42	0.1078	0.1719	0.01983	0.121	0.234	0.302
43	0.8550	0.1783	0.00372	0.093	0.099	0.106
44	0.5060	0.4098	0.01021	0.107	0.112	0.143
45	0.6480	2.7303	0.03483	0.142	0.148	0.148
46	0.1756	0.4393	0.06076	0.147	0.193	0.41
47	0.7030	0.8364	0.00368	0.156	0.156	0.156
48	0.3650	0.4870	0.04411	0.132	0.159	0.331
49	0.3223	0.3048	0.02420	0.1	0.111	0.228
50	0.5920	0.2405	0.00086	0.162	0.162	0.162
51	0.7827	0.3852	0.00868	0.117	0.117	0.132
52	0.2373	0.2968	0.05056	0.177	0.33	0.435
53	0.9493	0.1828	0.00951	0.128	0.152	0.213
54	0.2050	0.2300	0.03920	0.138	0.319	0.402
55	0.5100	0.0985	0.00426	0.148	0.186	0.207
56	0.7500	0.13011	0.01151	0.176	0.198	0.299
57	0.3585	0.39988	0.05149	0.147	0.204	0.317
58	0.1980	0.32169	0.02493	0.279	0.305	0.374
59	1.1467	0.43768	0.00273	0.166	0.166	0.166
60	1.0925	0.11300	0.00300	0.157	0.168	0.203
61	0.7450	0.06048	0.00122	0.158	0.163	0.185
62	0.1850	0.46792	0.00258	0.147	0.147	0.147
63	0.2125	0.40027	0.07341	0.135	0.356	0.447
64	0.4544	0.30339	0.09608	0.14	0.243	0.55

65	1.0251	1.00427	0.00504	0.16	0.16	0.16
66	0.2450	0.17985	0.00053	0.14	0.142	0.147
67	0.6953	0.30558	0.03298	0.113	0.125	0.184
68	0.1850	0.07679	0.00371	0.163	0.199	0.241
69	0.7300	0.10265	0.00135	0.155	0.164	0.175
70	4.9550	0.00338	0.00001	0.087	0.087	0.087
71	0.8777	0.12255	0.00225	0.1	0.106	0.133
72	0.2719	0.44484	0.07759	0.127	0.189	0.468
73	0.2600	0.17786	0.01835	0.158	0.194	0.4
74	0.3083	1.05520	0.12332	0.126	0.154	0.319
75	1.0055	0.63264	0.03579	0.147	0.168	0.224
76	0.7200	0.05849	0.00556	0.137	0.2	0.269
77	1.1221	0.41380	0.00371	0.131	0.135	0.135
78	0.4406	0.78881	0.00830	0.154	0.154	0.154
79	0.7095	1.09797	0.02213	0.163	0.163	0.163
80	1.0983	0.45837	0.05211	0.156	0.196	0.33
81	0.8193	1.80641	0.01404	0.162	0.162	0.167
82	0.0000	0.31950	0.00000	0.15	0	0
83	0.2000	0.08873	0.02263	0.161	0.387	0.529
84	0.6139	1.45468	0.01255	0.138	0.142	0.142
85	0.6978	0.23475	0.00847	0.121	0.141	0.181
86	0.5100	0.10504	0.00996	0.154	0.228	0.303
87	1.0019	0.14026	0.00946	2.33	2.387	2.44
88	0.2333	0.09609	0.00619	0.156	0.212	0.233
89	0.2200	0.27375	0.04397	0.149	0.335	0.395
90	0.0000	0.18860	0.00000	0.158	0	0
91	0.8463	0.55784	0.05021	0.137	0.16	0.301
92	0.4433	0.05232	0.00183	0.145	0.159	0.17
93	0.2733	0.15518	0.01032	0.148	0.178	0.233
94	1.1757	0.15816	0.01139	0.166	0.193	0.254
95	0.7907	0.14642	0.01210	0.126	0.198	0.291